Composites: Part A 151 (2021) 106671

Contents lists available at ScienceDirect

Composites Part A

journal homepage: www.elsevier.com/locate/compositesa

Compressible and robust PANI sponge anchored with erected MXene flakes for human motion detection

Kangqi Chang [a], Le Li [a], Chao Zhang [b], Piming Ma [a], Weifu Dong [a], Yunpeng Huang [a,*], Tianxi Liu [a,*]

[a] Key Laboratory of Synthetic and Biological Colloids, Ministry of Education, School of Chemical and Material Engineering, Jiangnan University, Wuxi 214122, China
[b] State Key Laboratory for Modification of Chemical Fibers and Polymer Materials, College of Materials Science and Engineering, Donghua University, Shanghai 201620, China

ARTICLE INFO

Keywords:
A. Foams
A. Smart materials
A. Nanocomposites
B. Electrical properties

ABSTRACT

Advanced pressure sensors featuring high compressibility, high sensitivity, fast response time, and superior stability have attracted tremendous research attention because of their potential applications in artificial intelligence technology and wearable electronics. In this work, a robust sponge-like piezoresistive pressure sensor with remarkable elasticity and high sensitivity was fabricated by anchoring perpendicularly oriented MXene flakes on polyaniline (PANI) wrapped polymeric sponge via freeze-drying-assisted depositing strategy. Owing to the stable 3D conducting networks provided by PANI sponge and the intimate electrical contact between erected MXene flakes upon subtle deformation, good sensitivity, wide working range, low detection limit, fast response and recovery times, and excellent durability can be simultaneously obtained. Furthermore, various physiological activities (speech recognition, swallowing, joint movement, etc.) can also be detected in real-time and wireless manner by the flexible MXene/PANI sponge sensors, demonstrating their great potential in low-cost and high-performance wearable piezoresistive pressure sensing devices.

1. Introduction

Recent advances in electronic skins (E-skins), wearable medical devices, soft robotics, human–machine interaction technology have stimulated tremendous research interests in wearable electronics [1–5]. Flexible sensors are the major components of artificial wearable electronic devices, which include pressure sensors, temperature sensors, gas sensors, humidity sensors and gravity sensors, etc. Amongst, the pressure sensors have attracted more research attention in wearable electronic fields due to their wide applications [6,7]. Flexible pressure sensors with high sensitivity are capable of sensing and detecting a wide variety of human movements, including small motions like speaking, heartbeat, and wrist pulse, as well as major movements like joint bending and muscle movements [8–11]. Generally, pressure sensors can be categorized into four types depending on their work mechanisms: piezoresistive, piezoelectric, frictional, and capacitive [12–14]. Amongst, piezoresistive pressure sensors have been widely studied due to their advantages of low cost, fast response time, and flexible deformation advantages [15–17]. Current piezoresistive pressure sensors made from elastic substrates and conductive materials including metal nanowires [18–20], nanoparticles [21], organic macromolecule [22], and ceramics [23] always suffer from narrow working range and uncontrollable susceptibility, which cannot meet the strict requirements of flexible/wearable pressure sensors. Therefore, the development of piezoresistive pressure sensors with high sensitivity, high compressibility, and fast response time remains a barrier for their further application.

Recently, three-dimensional (3D) foam/aerogel materials with good electrical conductivity and elasticity have emerged as ideal candidates for lightweight and flexible piezoresistive strain/pressure sensors [24–26]. In particular, carbon foam/aerogels composed of carbon nanofibers (CNFs), carbon nanotubes (CNTs), and graphene building blocks exhibit favorable pressure sensing performance due to their excellent mechanical properties and high conductivity. For example, Qiu et al. reported an ultralight graphene aerogel with functional nanoscale cellular architectures by a freeze-casting process, which exhibited high sensitivity (0.23–10 kPa^{-1}) and ultralow detection limit (0.082 Pa) when used flexible piezoresistive sensor [27]. Wang and coworkers fabricated an all-carbon foam with stable resistance and

* Corresponding authors.
E-mail addresses: hypjnu@jiangnan.edu.cn (Y. Huang), txliu@jiangnan.edu.cn (T. Liu).

https://doi.org/10.1016/j.compositesa.2021.106671
Received 20 August 2021; Received in revised form 26 September 2021; Accepted 2 October 2021
Available online 7 October 2021

excellent elasticity consisting of joint-welded CNTs, due to the junctions between CNTs in the cross-linked 3D conducting networks, obtained CNTs foam exhibited outstanding electrical, mechanical properties, and good stability over 1000 cycles [28]. However, due to the inherent mechanical rigidity and fragility of carbon-based foams/aerogels, the conductive carbon network can be easily impaired during large-scale and long-term compression, resulting in deformations and severe/irreversible deterioration in electrical conductivity, thus severely impede their sensitivity and compressibility. For these reasons, commercial polymer sponges/foams (e.g., PU, melamine, cellulose) with great elasticity, low density, and low cost are highly preferable for the large-scale fabrication of high-performance flexible pressure sensing materials. To improve the electrical conductivity of polymer substrates, carbon nanomaterials (activated carbon, CNTs, graphene, etc.) and conducting polymers (PPy, PANI, PEDOT:PSS, etc.) were always utilized as conductive fillers/coatings. For example, Li et al. reported the preparation of flexible pressure sensors backboned with chitosan (CS) treated polyurethane (PU) sponge, which was coated with negatively charged $Ti_3C_2T_x$ MXene sheets, obtained MXene/CS/PU piezoresistive sensor exhibited good compressibility and stable piezoresistive response for compressing strain up to 85% with the stress of 245.7 kPa [29]. However, it still remains a great challenge to simultaneously obtain a wide sensing range and high sensitivity for a piezoresistive pressure sensor due to the inevitable competition between compressibility and resistance change (electrical conductivity increases greatly under high compression, results in minute resistance change, i.e., low sensitivity).

Herein, a flexible pressure sensor with both high sensitivity, large compressibility, and fast response time is developed based on a 3D macroporous MXene/PANI functionalized polymeric sponge. Via the in-situ polymerization of PANI on melamine sponge to obtain a conductive and elastic skeleton, a freeze-drying-assisted depositing strategy is subsequently employed to deposit mono-layered MXene nano-flakes on the conductive sponge (as vividly illustrated in Fig. 1A). Prepared MXene/PANI sponge possesses 3D inter-connected conducting networks and excellent mechanical properties to maintain an intact conducting path under large-scale deformation. Especially, MXene nano-flakes perpendicularly deposited on PANI sponge during the vertical growth of ice crystal can ensure fast and large current change upon subtle deformation. As a result, prepared MXene/PANI sponge sensors show high sensitivity, fast response (80 ms), and great repeatability (5000 cycles), which can monitor both tiny body activities (speech recognition, swallowing) and large human motions (finger bending, elbow and knee movement) with a high signal-to-noise ratio (SNR), presenting their great potential in the application of new-generation wearable sensing devices.

2. Experimental

2.1. Materials

Aniline, concentrated hydrochloric acid (HCl) and ammonium persulfate (APS) were supplied by Sinopharm Chemical Reagent Company. Ti_3AlC_2 powder (200 mesh) was provided by Jilin 11 Technology Co., Ltd., China. Melamine sponge and Lithium fluoride (LiF) were bought from Aladdin. All the chemicals were used as obtained.

2.2. Synthesis of $Ti_3C_2T_x$ MXene

$Ti_3C_2T_x$ MXene was first synthesized through the MILD etching strategy. Typically, 1.5 g of LiF and 30 mL of 9 M HCl were mixed by magnetic stirring in a Teflon beaker. Subsequently, 1.5 g of Ti_3AlC_2 powders were slowly added to the above mixture solution and the etching reaction was carried out in a 35 °C water bath under mild stirring for 24 h to remove the intermediate Al atoms. After that, the

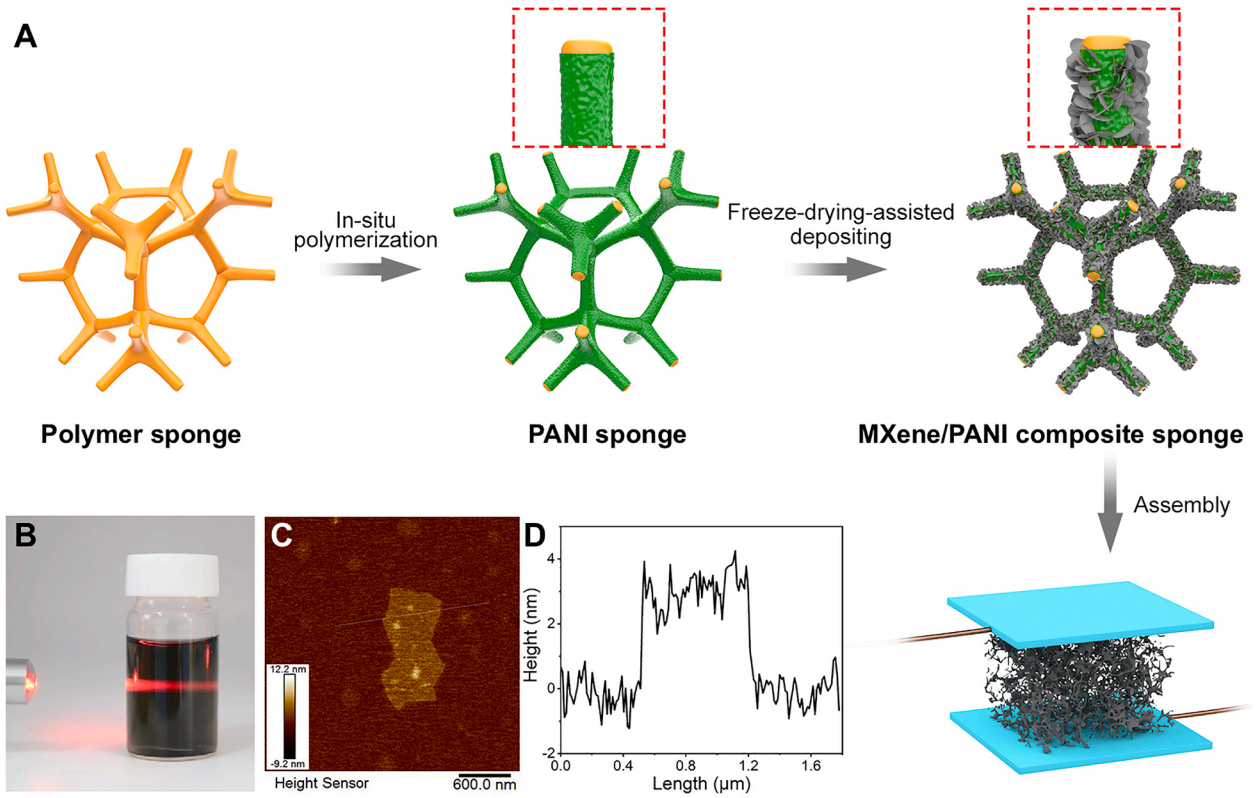

Fig. 1. (A) Fabrication process of MXene/PANI composite sponge. (B) Digital photograph of $Ti_3C_2T_x$ MXene dispersion. (C) AFM image and (D) corresponding height distribution of mono-layered $Ti_3C_2T_x$ MXene flake. (For interpretation of the references to colour in this figure legend, the reader is referred to the web version of this article.)

product was continuously washed with deionized water followed by centrifugation until the pH of the supernatant was neutral. Finally, exfoliation was performed under ultrasonication in nitrogen flow and ice bath to obtain a stable $Ti_3C_2T_X$ MXene suspension.

2.3. Fabrication of MXene/PANI composite sponge

First of all, the commercial melamine sponge (1.661 g cm^{-3}) was divided into thin slices (1.5 × 1.5 × 0.5 cm^3), followed by washing with deionized water and alcohol for several cycles. Thereafter, an in-situ polymerization in an ice bath was employed to fabricate PANI sponges. Briefly, the washed melamine sponge was first immersed in HCl solution (0.1 M, 50 mL) containing aniline (0.03–0.09 M) for 4 h to ensure effective adsorption, then 20 mL of HCl solution (0.1 M) containing APS (0.015–0.045 M) was slowly dropped in the above solution to initiate the polymerization. The reaction time for in-situ polymerization of PANI was set as 8 h with an ANI/APS molar ratio kept at 2:1. The obtained PANI sponge was then washed with deionized water and dried in a vacuum oven at 60 °C. A freeze-drying-assisted depositing strategy was subsequently applied to prepare the MXene/PANI composite sponge. Briefly, freshly-prepared PANI sponge was first immersed in the MXene suspension (5 mg ml^{-1}) for 10 s for the complete infiltration of MXene inside voids, followed by freezing in a stainless-steel bottomed vessel in −70 °C alcohol, and then lyophilized for 1 h to obtain MXene/PANI composite sponge.

2.4. Assembly of wearable pressure sensors

As-prepared MXene/PANI composite sponge with the size of 1.5 × 1.5 × 0.5 cm^3 was sandwiched with conductive tapes on both top and bottom surfaces, and then the piezoresistive pressure sensor was constructed via attaching copper wires on the conductive tapes. Finally, the sensor was encapsulated with translucent medical adhesive tapes to avoid the fluctuation of the current signal caused by environmental influence (as shown in Fig. 1).

2.5. Materials characterization

The lateral size and thickness of $Ti_3C_2T_x$ MXene sheets were characterized by the atomic force microscope (AFM, Bruker Dimension Icon). The morphologies of melamine sponge, PANI sponge, and MXene/PANI composite sponge were characterized using a scanning electron microscope (HITACHI S-4800). The chemical structures of the samples were confirmed by Fourier transformation infrared (FTIR) spectroscopy (Nicolet 6700). X-ray diffraction (XRD) patterns were collected using a Bruker D2 PHASER X-ray diffractometer with a Cu Ka X-ray source (λ = 1.5406 Å). The mechanical properties were investigated using an electronic universal testing machine (UTM2203, load cell = 50 N, Shenzhen Suns Technology Stock Co. Ltd, China). The measuring apparatus for pressure response was mainly made up of three components: a stress gauge (M5-2) for real-time pressure identification, a supportive base to hold the piezoresistive pressure sensor, and a stretchable stage (ESM303, Mark-10) for applying different pressure. The electrical signals of the pressure sensors under various pressures were recorded by an electrochemical workstation (CHI660E, Shanghai Chenhua Inc.).

3. Results and discussion

As shown in Fig. 1B, the homogeneous dark green dispersion of $Ti_3C_2T_x$ exhibits a typical Tyndall phenomenon when irradiated with a laser pointer. Further AFM images reveals the MXene sheets have an average thickness of ~3 nm and a lateral size of ~0.79 μm (Fig. 1C and D), demonstrating the successful synthesis of mono-layered MXene flakes. A commercial melamine sponge is regarded as a suitable compressible matrix for the fabrication of pressure sensors due to its cost-effectiveness and excellent mechanical properties, whereas, the innate insulativity greatly impedes its applications. In this work, in situ polymerization of PANI was conducted to endow the pristine polymer sponge with electrical conductivity. Fig. 2A and D shows the SEM images of the microporous architecture of the melamine sponge at low and high magnifications, the skeleton surface appears to be smooth in the magnified SEM image, and the pore diameters between the cross-linked skeletons are found to be about 100 μm. The white melamine sponge turned into dark green after the polymerization of PANI (inset of Fig. 2A and B). When the aniline concentration was 0.03 M, only a desultory PANI layer formed on the sponge surface (Fig. S1A). With the aniline concentration increased to 0.06 M, PANI particles can be seen uniformly wrapped on the surface of the melamine sponge without any aggregations (Fig. 2E). Further increasing the aniline concentration to 0.09 M, the system became unstable due to the fast reaction speed, resulting in the severe aggregation of PANI particles (Fig. S1B). Hence, the PANI sponge prepared with 0.06 M aniline concentration was selected as the optimized matrix for further treatment. Besides, Fig. 2B indicates the macroporous structure and the 3D interconnected skeleton of melamine sponge are fully reserved, verifying the superior mechanical stability and structural integrity of the polymeric sponge. Following that, a freeze-drying-assisted depositing strategy was utilized to deposit MXene flakes on the PANI sponge. As presented in Fig. 2C, the PANI sponge shows no shrinkage or collapse after treatment under extremely low temperature, and the MXene nanosheets were tightly assembled on the sponge skeleton in absence of any aggregation. Interestingly, the deposited MXene flakes all present the perpendicular orientation (Fig. 2F), which may stem from the directing of ice crystals during the freeze-drying process. It is notable that the erected MXene flakes are highly helpful in expanding the conductive contact area during the compressing process, which may greatly reinforce the sensitivity, response time and detect limits when used as piezoresistive strain sensors. In addition, almost all the microporosity of the sponge is retained after deposition of PANI and MXene, thus provide ample space for large-scale compression. The elemental mappings of the MXene/PANI composite sponge further confirm the uniform distribution of C, N, and Ti elements (Fig. 2G), demonstrating the successful deposition of PANI and MXene on the polymeric sponge backbone.

The chemical structure of the PANI sponge and original melamine sponge were characterized by FTIR (Fig. 3A). The peak of melamine sponge at 1541 cm^{-1} corresponds to the C═N stretching vibration, the peak at 972 cm^{-1} can be readily indexed to the ether bridge (—CH_2—O—CH_2—), and the sharp absorption peak located at about 810 cm^{-1} is attributed to the triazine ring in melamine sponge [30,31]. For the spectrum of PANI coated sponge, the absorbance at 787 cm^{-1} corresponds to the C—H stretching vibration on the benzene ring of PANI. Further XRD measurements were performed to investigate the detailed crystal structures of the samples (Fig. 3B). It is obvious that the amorphous peak of melamine can be observed in the patterns of all sponge samples. The absence of PANI peaks is ascribed to its relatively low diffraction intensity. The characteristic peak of the MXene located at 8.1° corresponded to the (0 0 2) crystal plane of the MXene, which can be clearly identified in the pattern of MXene/PANI sponge, indicating the successful incorporation of MXene [32–34]. Meanwhile, the (0 0 2) characteristic peak of the MXene shifts from 8.1° to 7.7° after depositing on PANI sponge, which can be ascribed to the enlarged interlayer spacing of MXene layers during freeze-drying process.

Good flexibility and compressibility are crucial properties in determining the operation ranges of flexible pressure sensors, which allow the sensors to bending/straightening or compressing/releasing upon stimuli without being damaged. Fig. 4A shows that the original melamine sponge displays excellent elasticity with high compressibility of 80%, which laid a solid basis for the preparation of MXene/PANI composite sponge with great compressibility and structural stability. Interestingly, the stress–strain curves of the neat melamine sponge show three linear ranges. To start with, the compression stress rises linearly and fast when the strain is less than 10%, then increases steadily with a lower slop at

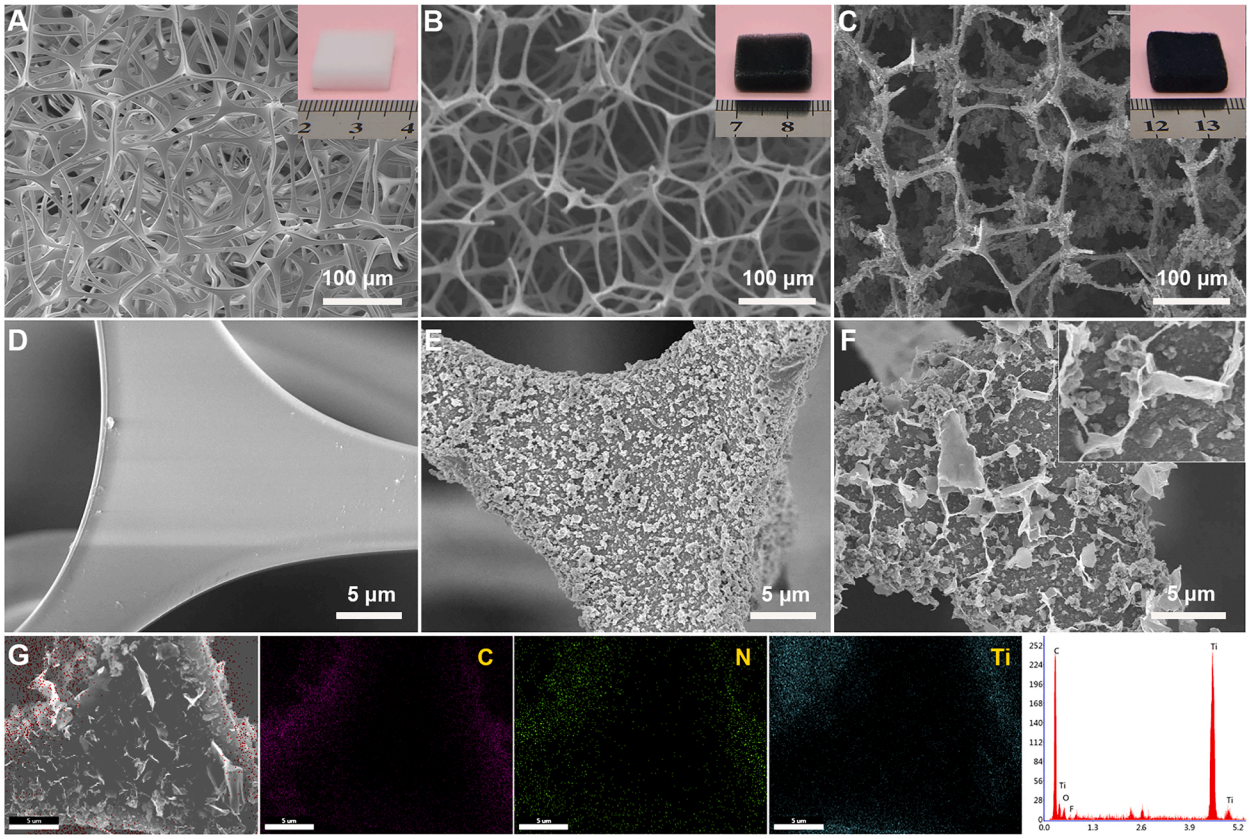

Fig. 2. SEM images of obtained samples at different magnifications: (A, D) melamine sponge, (B, E) PANI sponge, and (C, F) MXene/PANI composite sponge, respectively. (G) Elemental mapping of MXene/PANI composite sponge. (For interpretation of the references to colour in this figure legend, the reader is referred to the web version of this article.)

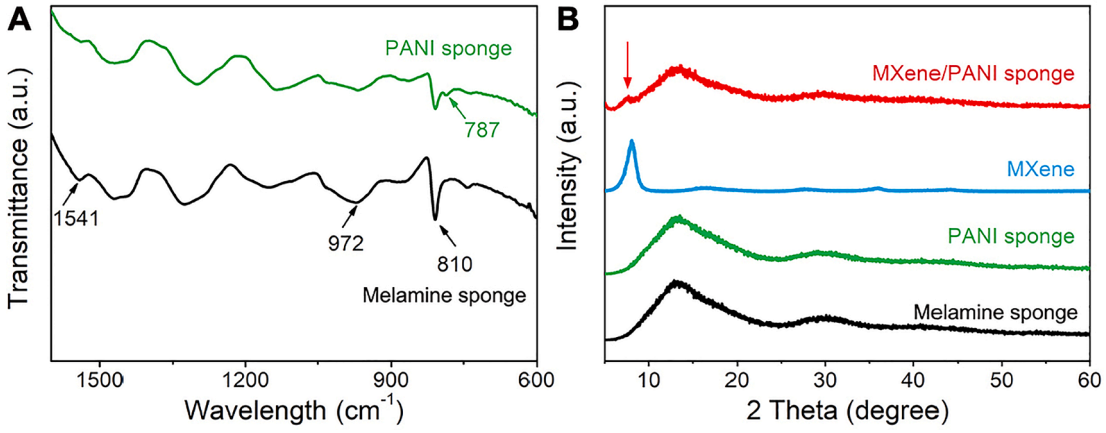

Fig. 3. (A) FTIR spectra of melamine sponge and PANI sponge. (B) XRD patterns of melamine sponge, PANI sponge, $Ti_3C_2T_x$ MXene, and MXene/PANI composite sponge, respectively. (For interpretation of the references to colour in this figure legend, the reader is referred to the web version of this article.)

the strain range of 10–60%. Specifically, stresses values of the melamine sponge at 40% and 60% strain are 9.7 and 12.2 kPa, respectively. Since most of the sponge skeletons have reached compact contact as the strain exceeds 60%, further compression results in the quick increment of stress, which is 17.05 kPa at 80% compression. The stress–strain curves of the PANI sponge and MXene/PANI composite sponge are similar to those of the melamine sponge. Specifically, the PANI sponge exhibits relatively lower pressure values at lower strains (<60%) (Fig. 4B). In addition, the MXene/PANI composite sponge exhibits enhanced mechanical strength than those of neat melamine sponge and PANI sponge, the maximum compressive stress values at 20, 40, 60, and 80% strains are 3.96, 6.75, 10.79, and 21.51 kPa, respectively (Fig. 4C). The stress–strain curve of MXene/PANI composite sponge is less obvious than melamine sponge in the three-stage linear configuration, which may be caused by the "soften" effect of PANI coating. Meanwhile, all the compressive stress–strain curves show obvious hysteresis, which is attributed to the inevitable energy loss during compression of the macroporous sponge. Notably, the gap between the compressing and releasing curves of MXene/PANI sponge is smaller than those of the other two sponges, indicating the improved mechanical properties of the MXene/PANI composite sponge [8]. It is also worth mention that the typical pressure of normal human activities is divided into three states:

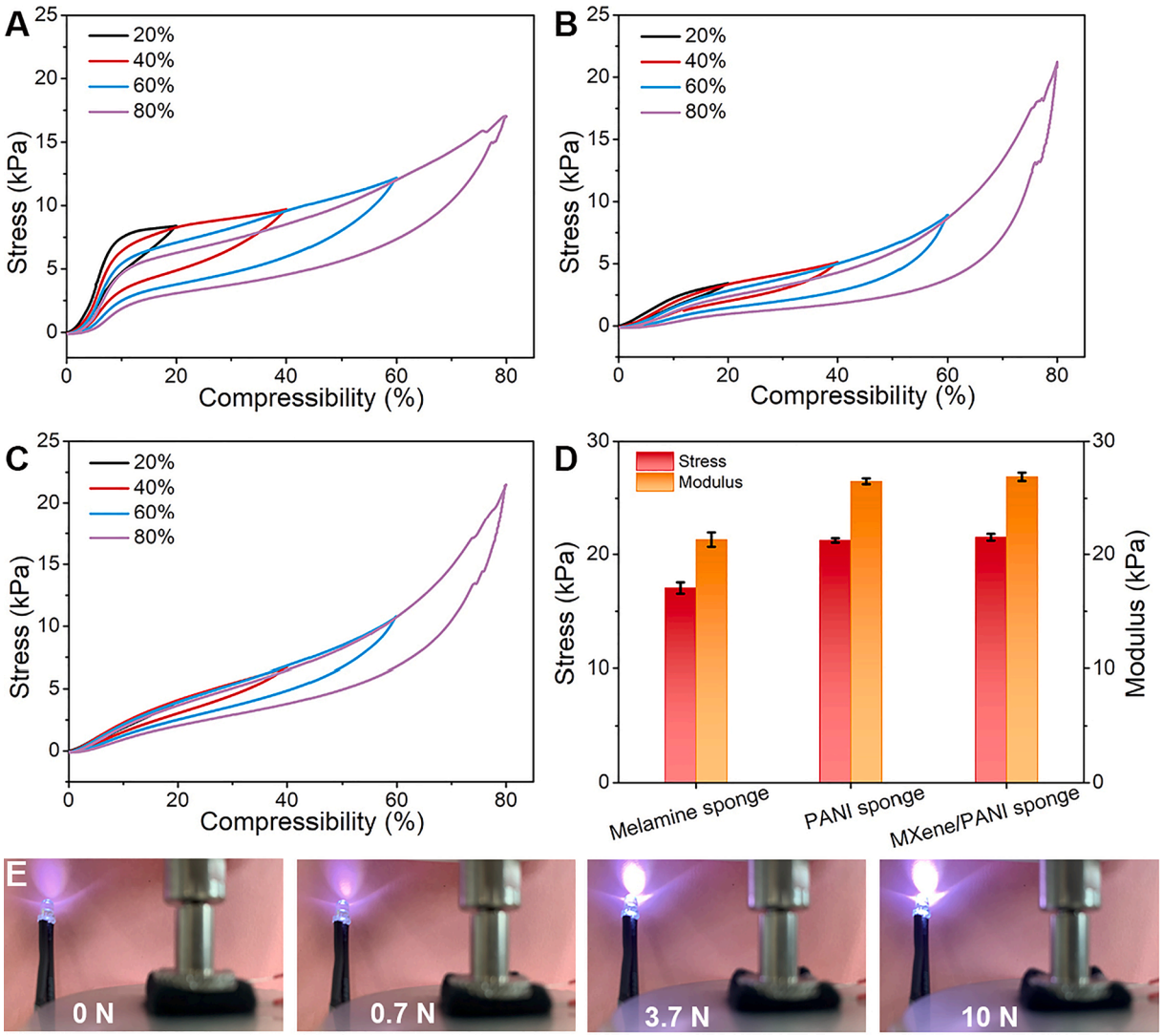

Fig. 4. The compressive stress–strain curves of (A) melamine sponge, (B) PANI sponge, (C) MXene/PANI composite sponge, and (D) comparison on the modulus of three samples. (E) Demonstration showing the conductivity of MXene/PANI composite sponge. (For interpretation of the references to colour in this figure legend, the reader is referred to the web version of this article.)

tiny pressure at 1 Pa–1 kPa (e.g., human skin perception), low-pressure range of 1–10 kPa (e.g., mild click), and the medium-pressure state at 10–100 kPa (e.g., joint movement). The MXene/PANI composite sponge exhibits the wide strain (0–80%) and stress (0–27 kPa) ranges, empowering itself with capabilities to detect various human activities. Comparison on the mechanical properties between three aerogels indicates the incorporation of PANI and MXene can help enhance the strength and modulus of the composite aerogel (Fig. 4D). In addition, a power source and an LED lamp were connected with the MXene/PANI composite sponge to demonstrate its possible application for piezoresistive pressure sensor (Fig. 4E). Interestingly, the brightness of the bulb can be adjusted in real-time by compressing the MXene/PANI composite sponge, indicating the fast establishment of conducting network in the elastic skeleton.

The excellent elasticity and conductivity of the MXene/PANI composite sponge prompt us to further explore its piezoresistive pressure sensing performance. As indicated in Fig. 5A, the I-V curves under various pressures exhibit good linearity, implying the efficient ohmic contact within the microporous sponge. Fig. 5B and C show the changes of current versus applied pressure for the PANI sponge and the MXene/PANI composite sponge in pressure range of 0–23 kPa, respectively. The slope of the plot can be calculated according to the following equation to define the sensitivity of pressure sensors.

$$S = \frac{\Delta I}{I_0 \Delta P} = \frac{(I - I_0)}{I_0 \Delta P}$$

where P represents the applied pressure, I denotes the current when pressure is applied, and I_0 is the current when no pressure is applied. The MXene/PANI composite sponge-based piezoresistive pressure sensor showed various responses to the applied pressures. When the MXene/PANI sponge is squeezed, the corresponding relative currents of the sensor rise instantly with a two-step ascending process, which rises slowly in an ultra-low-pressure range below 7 kPa, resulting in sensitivity as high as 0.0832 kPa^{-1}. Then, the current change of MXene/PANI increases rapidly in the relatively higher-pressure range of 7–23 kPa with a significantly boosted sensitivity of 0.3106 kPa^{-1}. The current change curve of the PANI sponge presents a fairly similar trend as that of MXene/PANI composite sponge, yielding the sensitivities of 0.0285 kPa^{-1} in the low-pressure range, and a higher value of 0.2242 kPa^{-1} in the high-pressure range. Apart from these, PANI sponge deposited with non-oriented MXene flakes was also prepared by direct drying the sponge under ambient environment, which also manifests the two linear sensing range with the sensitivities of 0.0621 kPa^{-1} and 0.2349 kPa^{-1} in two pressure range (Fig. S2). It is notable that the sensitivity of the

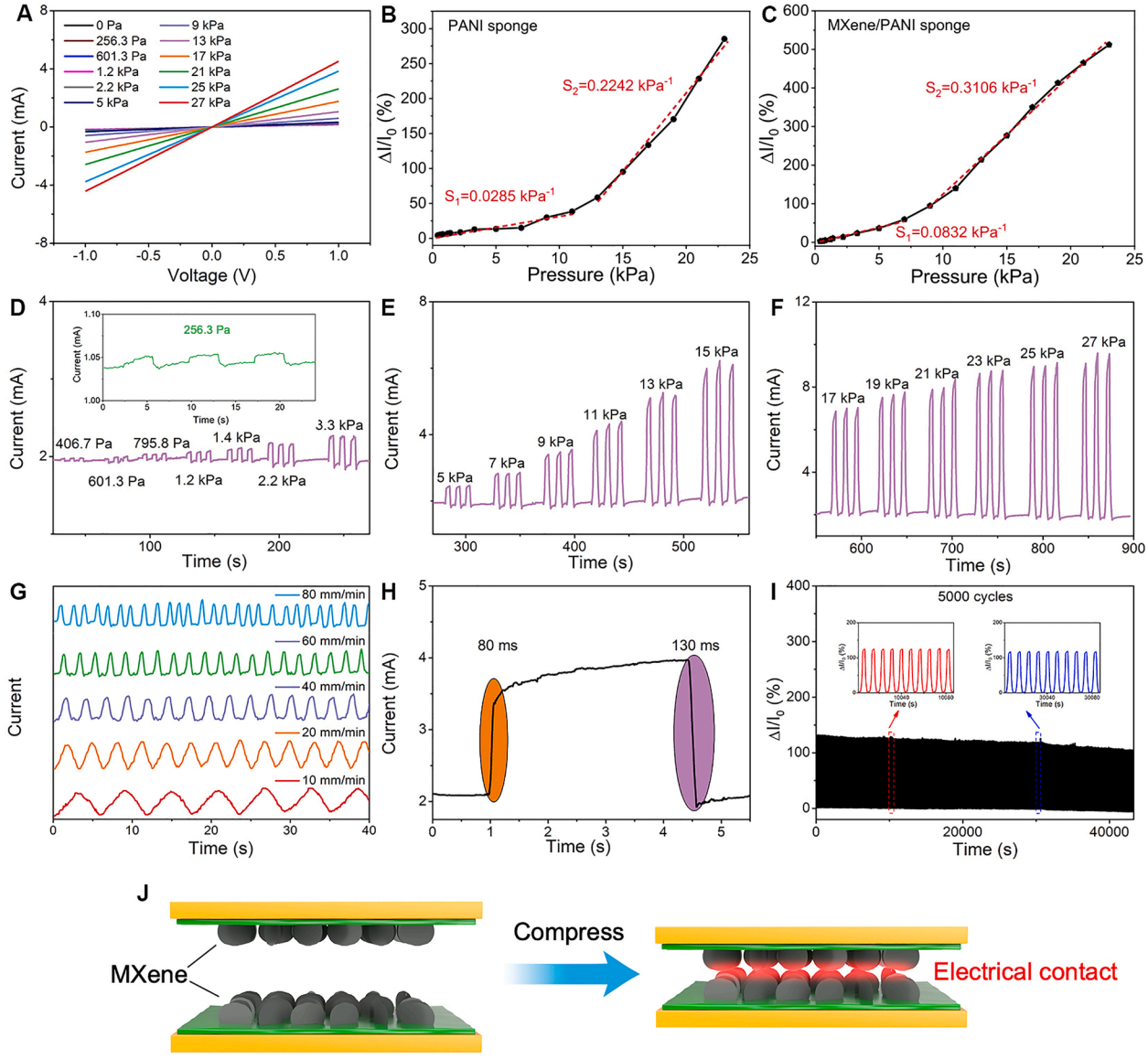

Fig. 5. (A) I-V curves of the MXene/PANI composite sponge. Sensitivity of the (B) PANI sponge and (C) MXene/PANI composite sponge piezoresistive pressure sensors. (D-F) I-T curves of the MXene/PANI composite sponge under various applied pressure. (G) Current response of the MXene/PANI composite sponge to forces with different speed. (H) Response and recovery time of the MXene/PANI pressure sensor. (I) Stability test of the pressure sensor, insets are the enlarged view of the response curves. (J) Schematic illustration for the improved sensitivity of the pressure sensor under external compression. (For interpretation of the references to colour in this figure legend, the reader is referred to the web version of this article.)

MXene/PANI composite sponge is largely enhanced compared to PANI sponge and non-oriented MXene deposited PANI sponge, indicating the perpendicularly oriented MXene flakes anchored on PANI wrapped elastic sponge could provide more intimate electrical contact, thus resulting in the higher sensitivity when subjected to the same pressure. The sensing performance was further compared with those of the previously published piezoresistive pressure sensors (as shown in Table S1), it is obvious that our designed MXene/PANI composite sponge manifests competitive sensitivity, sensing range and response/recovery time.

To further assess the pressure sensing performance of PANI sponge anchored with erected MXene flakes, relative current changes of the composite sponge are measured by applying stepwise increased external pressures. As reflected by the I-T curves in Fig. 5D–F, the on–off ratio increases well upon increasing the applied pressure, demonstrating the MXene/PANI sponge sensor can distinguish different levels of pressure, empowering the MXene/PANI composite sponge with potentials in complex pressure detecting applications. Meanwhile, it is apparent that the relative current change of the sensor is highly repeatable under the low, medium, and high-pressure ranges, confirming the stable sensing performance of MXene/PANI composite sponge. Additionally, the detection limit of MXene/PANI pressure sensor is determined as low as 256.3 Pa (inset of Fig. 5D). Stable response under multiple compressing rates is also very essential for the practical applications of sensors for complex pressure sensing. As shown in Fig. 5G, the MXene/PANI composite sponge shows a very steady current response under all compression rates. Besides, an instant pressure (800 Pa) under a high tensile rate (500 mm min^{-1}) was exerted to the MXene/PANI sponge sensor to determine its response and recovery time. As revealed in Fig. 5H, very rapid response and recover time of 80 ms and 130 ms are obtained, much faster than that of PANI sponge (300/400 ms, as shown in Fig. S3), the excellent responsiveness of the piezoresistive pressure sensor can facilitate its application in the real-time monitoring of human physiological signals. Apart from that, the MXene/PANI composite sponge also exhibits stable current change (Fig. 5I, current retention of 80%) and nearly intact perpendicular morphology (Fig. S4) after 5000 compressing/releasing cycles under 11 kPa, confirming the outstanding

reproducibility, durability, and stability of the MXene/PANI piezoresistive sensor. The slight decline of the relative current is caused by the inevitable destruction of conductive paths by the large-scale deformation. The remarkable piezoresistive pressure sensing properties of the MXene/PANI composite sponge can be attributed to the 3D conducting networks provided by PANI coated melamine sponge, as well as the numerous electrical contacts contributed by perpendicularly oriented MXene flakes (as vividly illustrated in Fig. 5J). The high sensitivity and fast response/recovery time render the conductive sponge with potential applications in wearable electronic devices.

Considering the flexibility and outstanding sensing performance of the MXene/PANI composite sponge, we further assess its possible applications for real-time recognition of various human activities. Hence, the composite sponge was directly attached to the muscle or joint to monitor the subtle motion caused by micro deformation. Firstly, the flexible device was bonded to the skin with a bandage to achieve synchronous identification of throat vibration. As displayed in Fig. 6A and B, significant and stable current signals can be observed when the volunteer repeatedly pronounced the word “Sensor” and “MXene”. Besides, MXene/PANI composite sponge piezoresistive sensor can be used to monitor the swallowing process when attached to the throat. As shown in Fig. 6C, the small muscle activity near the gullet exerts pressure on the flexible sensor when the volunteer performing the swallowing motion, resulting in the obvious and stable current changes with characteristic peaks. Apart from these, MXene/PANI pressure sensor also can be used to distinguish different gestures when adhering to the finger joints (Fig. 6D). Attributing to its fast response and recovery ability, the flexible sensor can instantly detect the joint bending and returns to its initial state when the wrist and elbow straighten (Fig. 6E and F). All these demonstrations evidence that the MXene/PANI pressure sensor can be used to detect micro and large human motions in real-time. In addition, to assess the possibility of MXene/PANI pressure sensor for applications in electronic skin, a large-area pressure sensor array was built by constructing a 3 × 3 matrix of the tailored composite sponge (Fig. 6G). As shown in Fig. 6H and I, the pressure signals can be detected independently when putting the palm on the sensor array (exerted force is 5 N), implying the potential applications of MXene/PANI pressure sensors in artificial electronic skin and soft robotics. To further exploit the potential of MXene/PANI pressure sensor in portable sensing applications, the composite sponge was connected in series with a microcircuit implanted with a Bluetooth system, which gathers and transmits the signals to a cell phone for the final recording. The fabricated sensor array was worn by a volunteer weighing 65 Kg, and was taped to the heel and wrist for wireless monitoring of various human activities (Fig. 7A). Fig. 7B–G presents the relative resistance change when the wireless sensor is used to monitor running, jumping, walking, squatting/rising, wrist bending, and wrist motion during door-opening. Surprisingly, the wireless sensor can function continuously by exporting stable and repeatable electrical signals. Therefore, the MXene/PANI sponge-based pressure sensor may have potential applications in

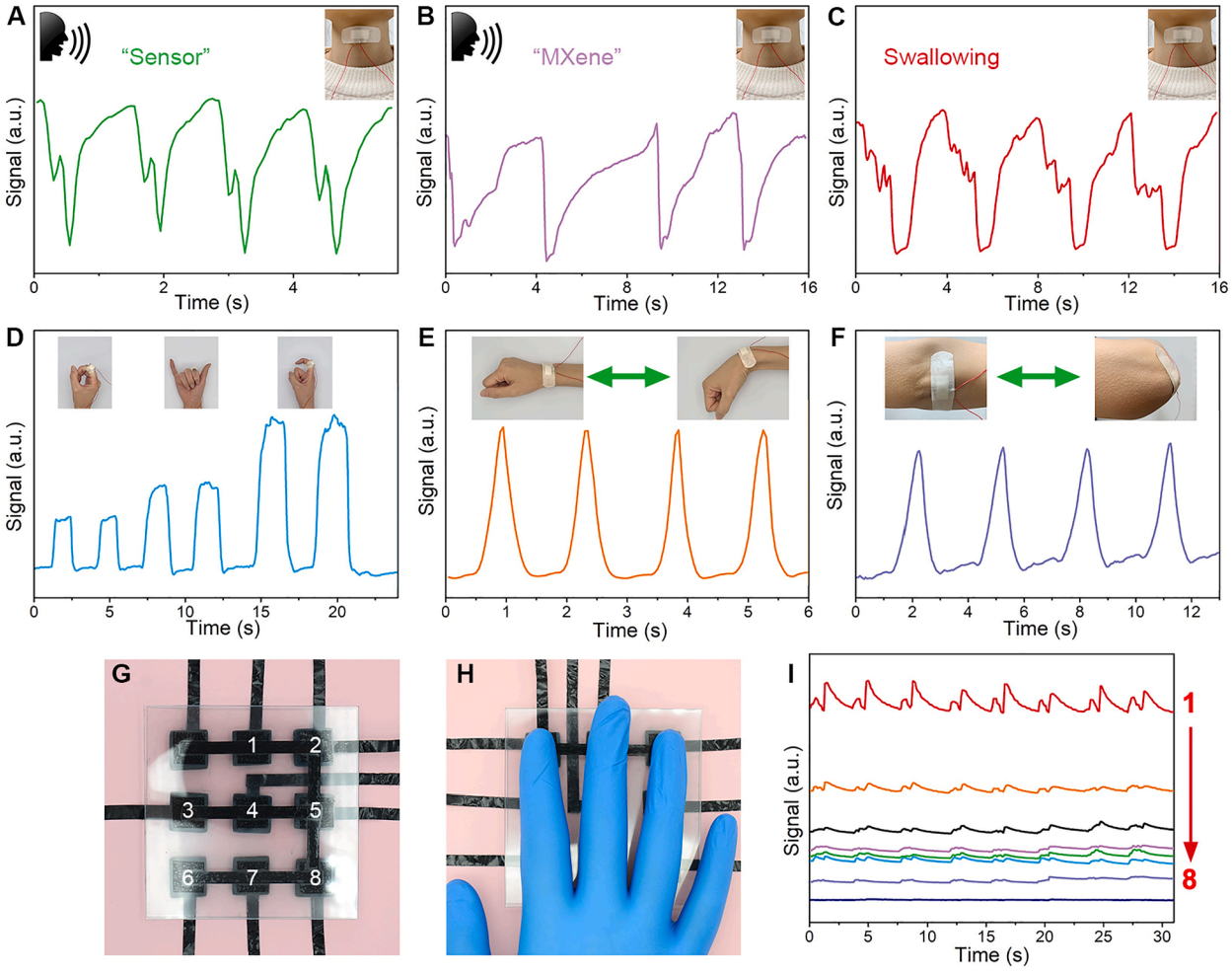

Fig. 6. Applications of the MXene/PANI based piezoresistive pressure sensor for the real-time detection of various human body activities: (A, B) Vocal cord vibration. (C) Swallowing. (D) Finger gestures. (E, F) Wrist and elbow bending/straightening. (G) Configuration of the 3 × 3 pixel array of the MXene/PANI sponge sensor. (H) A palm is pressing on the pixel array of sensors, and (I) corresponding pressure signal of individual pixel. (For interpretation of the references to colour in this figure legend, the reader is referred to the web version of this article.)

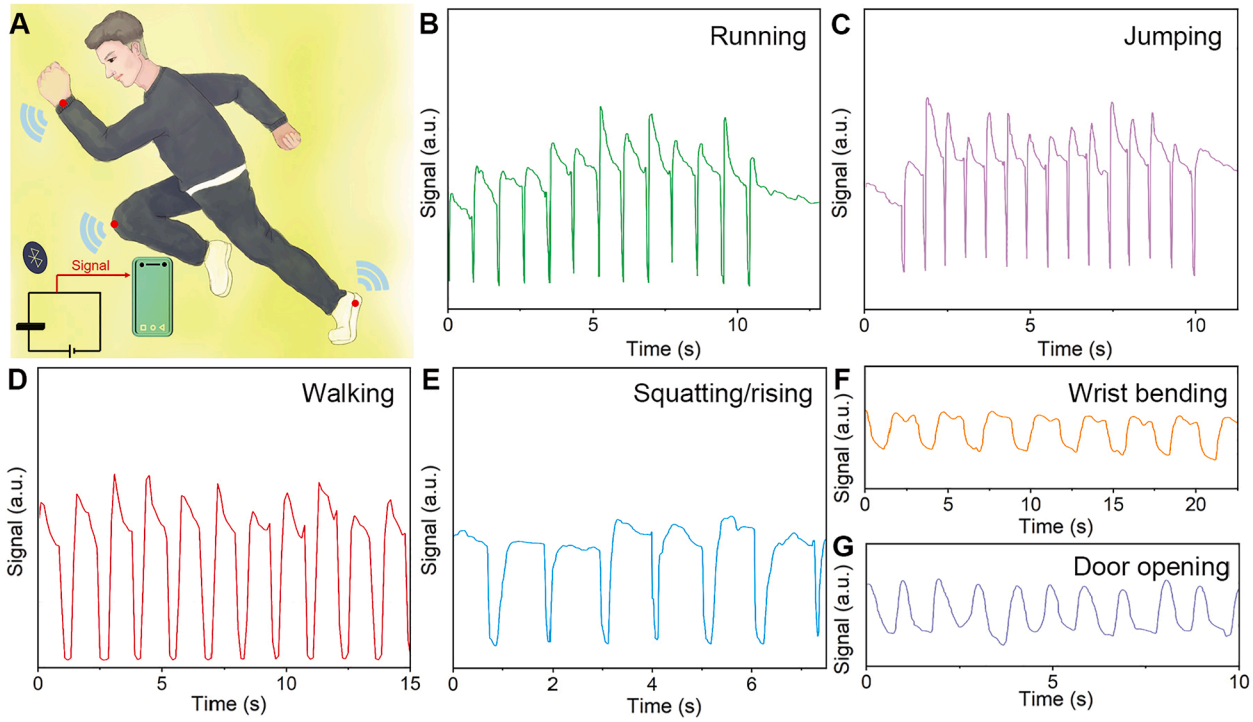

Fig. 7. (A) The MXene/PANI sponge sensor is connected to a circuit with Bluetooth module to wirelessly detecting various human motions: (B) Running, (C) jumping, (D) walking, (E) squatting and rising, (F) wrist bending, and (G) wrist motion during door-opening. (For interpretation of the references to colour in this figure legend, the reader is referred to the web version of this article.)

wireless wearable devices.

4. Conclusions

In conclusion, a compressible and robust MXene/PANI composite sponge anchored with perpendicularly oriented MXene flakes was rationally constructed via in-situ polymerization and freeze-drying-assisted depositing strategy. Combining the high compressibility and elasticity of polymeric sponge skeleton, the 3D inter-connected conducting PANI networks, and the intimate electrical contact between erected MXene flakes, as-designed composite sponge as a piezoresistive pressure sensor displays remarkable sensing performance in terms of a high sensitivity, a wide working range of 0–23 kPa, a low detection limit of 256.3 Pa, excellent sensing stability of 5000 compressing/releasing cycles under 11 kPa, and fast response and recovery times of 80 ms and 130 ms, respectively. As a result, the MXene/PANI sponge sensor also can be used to monitor a variety of human motions in real-time, exhibiting its great potentials in flexible/wearable electrics such as human–machine interaction, electronic skin, health-care monitoring, etc.

CRediT authorship contribution statement

Kangqi Chang: Methodology, Investigation, Writing – original draft. **Le Li:** Investigation, Data curation. **Chao Zhang:** Data curation, Validation. **Piming Ma:** Writing – review & editing. **Weifu Dong:** Writing – review & editing. **Yunpeng Huang:** Data curation, Validation, Supervision, Conceptualization, Writing – review & editing. **Tianxi Liu:** Conceptualization, Methodology, Supervision, Writing – review & editing.

Declaration of Competing Interest

The authors declare that they have no known competing financial interests or personal relationships that could have appeared to influence the work reported in this paper.

Acknowledgments

This work is financially supported by the National Natural Science Foundation of China (21875033), the Shanghai Scientific and Technological Innovation Project (18JC1410600), and the State Key Laboratory for Modification of Chemical Fibers and Polymer Materials, Donghua University.

Appendix A. Supplementary material

Supplementary data to this article can be found online at https://doi.org/10.1016/j.compositesa.2021.106671.

References

[1] Nela L, Tang J, Cao Q, Tulevski G, Han S-J. Large-area high-performance flexible pressure sensor with carbon nanotube active matrix for electronic skin. Nano Lett 2018;18(3):2054–9.
[2] Cai Y, Shen J, Ge G, Zhang Y, Jin W, Huang W, et al. Stretchable $Ti_3C_2T_x$ MXene/carbon nanotube composite based strain sensor with ultrahigh sensitivity and tunable sensing range. ACS Nano 2018;12(1):56–62.
[3] Tian M, Lu Y, Qu L, Zhu S, Zhang X, Chen S. A pillow-shaped 3D hierarchical piezoresistive pressure sensor based on conductive silver components-coated fabric and random fibers assembly. Ind Eng Chem Res 2019;58(14):5737–42.
[4] Mohammadifar M, Tahernia M, Yang JH, Koh A, Choi S. Biopower-on-skin: electricity generation from sweat-eating bacteria for self-powered e-skins. Nano Energy 2020;75:104994. https://doi.org/10.1016/j.nanoen.2020.104994.
[5] Bergner F, Dean-Leon E, Cheng G. Design and realization of an efficient large-area event-driven e-skin. Sensors-Basel 2020;20(7):1965.
[6] Gao W, Ota H, Kiriya D, Takei K, Javey A. Flexible electronics toward wearable sensing. Acc Chem Res 2019;52(3):523–33.
[7] Sui X, Downing JR, Hersam MC, Chen J. Additive manufacturing and applications of nanomaterial-based sensors. Mater Today 2021. https://doi.org/10.1016/j.mattod.2021.02.001.
[8] Yang T, Xie D, Li Z, Zhu H. Recent advances in wearable tactile sensors: materials, sensing mechanisms, and device performance. Mater Sci Eng R Rep 2017;115:1–37.

[9] Jiang C, Tan D, Sun N, Huang J, Ji R, Li Q, et al. 60 nm pixel-size pressure piezo-memory system as ultrahigh-resolution neuromorphic tactile sensor for in-chip computing. Nano Energy 2021;87:106190. https://doi.org/10.1016/j.nanoen.2021.106190.
[10] Zheng S, Ma J, Fang K, Li S, Qin J, Li Y, et al. High-voltage potassium ion micro-supercapacitors with extraordinary volumetric energy density for wearable pressure sensor system. Adv Energy Mater 2021;11(17):2003835. https://doi.org/10.1002/aenm.v11.1710.1002/aenm.202003835.
[11] Zhang Y, Wang L, Zhao L, Wang K, Zheng Y, Yuan Z, et al. Flexible self-powered integrated sensing system with 3D periodic ordered black phosphorus@MXene thin-films. Adv Mater 2021;33(22):2170174.
[12] Chen J, Zhu Y, Huang J, Zhang J, Pan D, Zhou J, et al. Advances in responsively conductive polymer composites and sensing applications. Polym Rev 2021;61(1):157–93.
[13] Wang C, Xia K, Wang H, Liang X, Yin Z, Zhang Y. Advanced carbon for flexible and wearable electronics. Adv Mater 2019;31(9):1801072. https://doi.org/10.1002/adma.v31.910.1002/adma.201801072.
[14] Wang Z, Jiang R, Li G, Chen Y, Tang Z, Wang Y, et al. Flexible dual-mode tactile sensor derived from three-dimensional porous carbon architecture. ACS Appl Mater Interfaces 2017;9(27):22685–93.
[15] Abdul Samad Y, Komatsu K, Yamashita D, Li Y, Zheng L, Alhassan SM, et al. From sewing thread to sensor: nylon® fiber strain and pressure sensors. Sensor Actuat B-Chem 2017;240:1083–90.
[16] liu H, Jiang H, Du F, Zhang D, Li Z, Zhou H. Flexible and degradable paper-based strain sensor with low cost. ACS Sustainable Chem Eng 2017;5(11):10538–43.
[17] Wu X, Han Y, Zhang X, Lu C. Spirally structured conductive composites for highly stretchable, robust conductors and sensors. ACS Appl Mater Interfaces 2017;9(27):23007–16.
[18] Jiang D, Wang Y, Li B, Sun C, Wu Z, Yan H, et al. Flexible sandwich structural strain sensor based on silver nanowires decorated with self-healing substrate. Macromol Mater Eng 2019;304(7):1900074. https://doi.org/10.1002/mame.v304.710.1002/mame.201900074.
[19] Shuai X, Zhu P, Zeng W, Hu Y, Liang X, Zhang Yu, et al. Highly sensitive flexible pressure sensor based on silver nanowires-embedded polydimethylsiloxane electrode with microarray structure. ACS Appl Mater Interfaces 2017;9(31):26314–24.
[20] Wu JM, Chen C-Y, Zhang Y, Chen K-H, Yang Ya, Hu Y, et al. Ultrahigh sensitive piezotronic strain sensors based on a $ZnSnO_3$ nanowire/microwire. ACS Nano 2012;6(5):4369–74.
[21] Si Y, Yu J, Tang X, Ge J, Ding B. Ultralight nanofibre-assembled cellular aerogels with superelasticity and multifunctionality. Nat Commun 2014;5(1):5802.
[22] Katsoulidis AP, He J, Kanatzidis MG. Functional monolithic polymeric organic framework aerogel as reducing and hosting media for Ag nanoparticles and application in capturing of iodine vapors. Chem Mater 2012;24(10):1937–43.
[23] Su L, Wang H, Niu M, Fan X, Ma M, Shi Z, et al. Ultralight, recoverable, and high-temperature-resistant SiC nanowire aerogel. ACS Nano 2018;12(4):3103–11.
[24] Long S, Feng Y, He F, Zhao J, Bai T, Lin H, et al. Biomass-derived, multifunctional and wave-layered carbon aerogels toward wearable pressure sensors, supercapacitors and triboelectric nanogenerators. Nano Energy 2021;85:105973. https://doi.org/10.1016/j.nanoen.2021.105973.
[25] Huang W, Li H, Zheng L, Lai X, Guan H, Wei Ye, et al. Superhydrophobic and high-performance wood-based piezoresistive pressure sensors for detecting human motions. Chem Eng J 2021;426:130837. https://doi.org/10.1016/j.cej.2021.130837.
[26] Wang H, Zhou R, Li D, Zhang L, Ren G, Wang Li, et al. High-performance foam-shaped strain sensor based on carbon nanotubes and $Ti_3C_2T_x$ MXene for the monitoring of human activities. ACS Nano 2021;15(6):9690–700.
[27] Qiu L, Bulut Coskun M, Tang Y, Liu JZ, Alan T, Ding J, et al. Ultrafast dynamic piezoresistive response of graphene-based cellular elastomers. Adv Mater 2016;28(1):194–200.
[28] Wang H, Lu W, Di J, Li Da, Zhang X, Li M, et al. Ultra-lightweight and highly adaptive all-carbon elastic conductors with stable electrical resistance. Adv Funct Mater 2017;27(13):1606220. https://doi.org/10.1002/adfm.v27.1310.1002/adfm.201606220.
[29] Li X-P, Li Y, Li X, Song D, Min P, Hu C, et al. Highly sensitive, reliable and flexible piezoresistive pressure sensors featuring polyurethane sponge coated with MXene sheets. J Colloid Interface Sci 2019;542:54–62.
[30] Bin D-S, Lin X-J, Sun Y-G, Xu Y-S, Zhang Ke, Cao A-M, et al. Engineering hollow carbon architecture for high-performance K-ion battery anode. J Am Chem Soc 2018;140(23):7127–34.
[31] Merline DJ, Vukusic S, Abdala AA. Melamine formaldehyde: curing studies and reaction mechanism. Polym J 2013;45(4):413–9.
[32] Wang J, Liu Y, Cheng Z, Xie Z, Yin L, Wang Wu, et al. Highly conductive MXene film actuator based on moisture gradients. Angew Chem Int Ed 2020;59(33):14029–33.
[33] Wang L, Zhang M, Yang B, Tan J, Ding X. Highly compressible, thermally stable, light-weight, and robust aramid nanofibers/Ti_3AlC_2 MXene composite aerogel for sensitive pressure sensor. ACS Nano 2020;14(8):10633–47.
[34] Song S, Yang H, Su C, Jiang Z, Lu Z. Ultrasonic-microwave assisted synthesis of stable reduced graphene oxide modified melamine foam with superhydrophobicity and high oil adsorption capacities. Chem Eng J 2016;306:504–11.